

WRIGHT FEDERAL AIRCRAFT LABORATORY
NATIONAL ADVISORY COMMITTEE FOR AERONAUTICS

SPECIAL REPORT No 136

YOU

THE EFFECT OF STREAMLINING THE AFTERBODY OF
AN N.A.C.A. COWLING

By George W. Stickle, John L. Crigler, and Irvin Naiman
Langley Memorial Aeronautical Laboratory

CLASSIFIED

Declassified in accordance with
NACA policy letter of Sept. 23, 1943

THIS DOCUMENT AND EACH AND EVERY
PAGE HEREIN IS HEREBY RECLASSIFIED
FROM Conf TO Unclass
AS PER LETTER DATED NACA Dec 23
Notice #122

December 1939

SR-136

THE EFFECT OF STREAMLINING THE AFTERBODY OF
AN N.A.C.A. COWLING

By George W. Stickle, John L. Crigler, and Irven Naiman

SUMMARY

The drag and the power cost associated with the changing of the nose of a nacelle from a streamline shape to a conventional N.A.C.A. cowling shape was investigated in the N.A.C.A. 20-foot tunnel. Full-scale propellers and nacelles were used. The increment of drag associated with the change of nose shapes was found to be critically dependent on the afterbody of the nacelle. Two streamline afterbodies were tested. The results of the tests with the more streamlined afterbody showed that the drag approached that of an airship form and that the added drag due to the open-nose cowling was only one-fourth of the drag increase obtained with the other afterbody. The results of this research indicate that the power cost, in excess of that with a streamline nose, of using an N.A.C.A. cowling in front of a well-designed afterbody to enclose a 1,500-horsepower engine in an airplane with a speed of 300 miles per hour amounts to 1.5 percent of the engine power. If the open-nose cowling is credited with 1 percent because it cools the front of the cylinders, the non-useful power cost amounts to only 0.5 percent of the engine power.

INTRODUCTION

The two primary functions of an engine cowling are:

- (1) To provide an engine enclosure of minimum drag.
- (2) To pump the cooling air through the engine or radiator.

Reference 1 points out that these functions may be treated separately because the definite amount of work required to be done on the cooling air is distinctly different from the ordinary aerodynamic drag of the cowling itself.

It is further shown in reference 1 that the drag

chargeable to pumping the air through the cowling is equal to the internal work (that is, the volume multiplied by the pressure drop) divided by the free-air velocity and the pumping efficiency. The pumping efficiency is shown to be nearly 100 percent for the high-speed condition. Tests with cooling air, the results of which are to be included in another report, show that this pumping efficiency can be obtained on set-up 2, which is the subject of this report. It is shown in reference 2 that a 550-horsepower engine operating with a temperature difference of 300° F. required approximately 1-1/2 percent of the engine power for internal cooling work. This internal work is utilized in cooling the rear of the engine cylinders. More modern engines with improved finning and baffling have reduced this value to about 1 percent of the engine power.

The problem of providing an engine enclosure that would have minimum drag was investigated in reference 1. The best design of the nose contour was determined as well as the best method of exhausting the cooling air. It was stated that the drag of the basic blunt-nose cowling shape of an air-cooled engine has a drag somewhat in excess of that of a more properly streamlined shape, such as an airship form. In order to ascertain the reason for this increase in drag, several cowling noses varying in contour and dimensions were investigated to determine the variable of the nose shape that made the drag of the open-nose cowling larger. At the beginning of this research, an afterbody similar to that of reference 1 was used but, when the design was copied, the expansion angle of the finished nacelle was slightly larger than that of the nacelle used in reference 1. This small change in the expansion angle gave a critical flow over the after part of the nacelle and the drag coefficient changed radically with the Reynolds Number. This undesirable condition focused attention on the shape of the afterbody and work was begun to design an afterbody that would not give a critical flow condition.

The problem of reducing the form drag of the afterbody of the nacelle is similar to the problem of designing the expansion side of a venturi tube. The air must be slowed down with the least loss of energy. If the expansion angle is too large, loss in energy occurs because the kinetic energy is not transformed into potential energy. If the expansion angle is too small, skin friction over the body will make the drag too high. Further study of

the effect of the shape of the afterbody on the drag is planned. If the cowling is placed in front of a wing that has a thickness equal to or larger than the nacelle diameter, or in front of a fuselage with a diameter equal to or larger than the nacelle diameter, the slowing down of the air is taken care of by the wing or fuselage contour. If the air that flows over the wing or fuselage is at no place expanded too rapidly, this source of cowling drag disappears.

The results of tests using the more streamlined afterbody are the subject of the present report. This report shows that, if the correct power chargeable to the drag of the nose opening is used, no reason exists, from considerations of aerodynamic efficiency only, ever to abandon the open-nose cowling for any other type of engine installation. This statement takes on added significance when it is realized, as is shown in references 1 and 3, that the open-nose cowling provides, at no measurable internal power loss, cooling for the front of the cylinder equivalent to approximately 70 percent of the cooling obtainable in the free air stream.

SYMBOLS

- V, velocity of the free air stream.
- ρ , air density.
- q, dynamic pressure of the air stream, $1/2 \rho V^2$.
- D, drag of the cowling-nacelle unit.
- D_o , drag of streamline shape.
- F, frontal area of the cowling, 14.75 square feet.
- C_D , drag coefficient, D/qF .
- C_{D_o} , streamline shape drag coefficient.
- R, net thrust of the propeller-nacelle unit.
- P, power input to propeller.
- η_n , net efficient of the propeller-nacelle unit, RV/P .

η_0 , net efficiency of the propeller-nacelle unit on the basic nose shape.

S, propeller disk area.

P_c , disk-loading coefficient or unit disk loading, P/qSV .

ΔC_D , effective change in drag coefficient caused by the nose shape, $(\eta_0 - \eta_n) P_c \frac{S}{F}$.

$1/\sqrt[3]{P_c}$, propeller disk-loading coefficient, $\sqrt[3]{\frac{\rho S}{2P}}$.

APPARATUS AND METHODS

The investigation was conducted in the N.A.C.A. 20-foot tunnel, which with its standard equipment is described in reference 4.

Figure 1 presents a line drawing of the arrangements tested, with the designations of the noses and the nacelles used in each arrangement. Set-up 1 was used in reference 1; set-up 2 was used in the present investigation. The nose shapes that were used in reference 1 are shown in figures 2 to 4. The results presented in this paper were obtained with a pointed tail as shown in figure 1 and not with the tail pump shown in figure 3. Figures 5 to 7 show the nose shapes used in the tests for this report. The results in this report were obtained with all slots closed and faired.

Because the engine-nacelle installation for a tractor propeller is located in the slipstream of the propeller, it is necessary to study the nacelle with the propeller operating to obtain the possible secondary effects of the propeller. In order to include as many details as possible with a reasonable number of tests, three selected 10-foot-diameter propellers were tested over a range of blade angles from 20° to 55° at the 75-percent radius. Propeller B is Navy plan form 4893 with airfoil sections near the propeller hub; propeller C is Navy plan form 5868-9 with the conventional round blade shanks near the hub. Both propellers B and C have a constant pitch distribution when set at a blade angle of 15° at the 75-percent radius. Propeller C_x is the same as propeller C except that it has a constant pitch distribution from the 50-percent radius to the tip when set at a blade angle of 35° at the 75-percent radius. Figure 8 shows one blade of each of the three 10-foot-diameter 3-blade propellers.

All the tests were made with zero air flow through the nacelle to eliminate the effect of cowling pumping efficiency on the results. The struts were shielded from the air stream as shown in figures 2 to 7. Because the tare drag remained constant for each set-up, the results are not corrected for this effect. The results are corrected, however, for the effect of horizontal buoyancy because this effect varies with the body shape and the location of the test arrangement in the tunnel. The magnitude of the effect of horizontal buoyancy can be seen in table I. Set-up 1 was located 2 feet farther forward in the tunnel than set-up 2. Inasmuch as the static pressure in the air stream increases toward the entrance cone, the buoyancy corrections for set-up 1 were larger than for set-up 2.

DISCUSSION OF FIGURES

The condensed results of the drag tests are given in table I. This table shows that the more streamlined after-body reduced the drag increment chargeable to the open-nose N.A.C.A. cowling, $C_D - C_{D_0}$, from 0.0350 to 0.0081.

The net efficiency was computed from the net force on the tunnel balance. The net efficiency for each test

was plotted against $1/\sqrt[3]{P_c}$ ($= \sqrt[3]{\frac{PS}{2F}}$). Envelopes were drawn from the composite of all the propeller tests for each arrangement. The net efficiency envelopes are shown in figures 9, 10, and 11. A comparison of the envelopes for any propeller at constant values of $1/\sqrt[3]{P_c}$ shows the power cost of the front opening of the cowling when in the presence of that propeller.

These propeller results strictly apply only to the ratio of F/S used in the test arrangement. If the value of F/S were larger, the effect of the nose opening would be somewhat greater than noted and, if smaller, the reverse would be true. Since the present trend is to put more engine power into the same engine diameter, this ratio has been decreasing because the greater engine power requires larger propeller diameters. The test arrangement is near the upper end of the range of F/S used and, consequently, the effect of the nose opening discussed in this report is larger than will be experienced in most modern installations.

The change in the net efficiency may be defined as

$$\eta_o - \eta_n = \frac{\Delta C_D}{P_c} \frac{F}{S}$$

where ΔC_D is the effective change in the drag coefficient caused by the nose shape. The curves used as the basis of comparison are designated η_o curves. The η_o curves for propellers C and C_x were obtained with nose 4, and the η_o curve for propeller B was obtained with nose 5 and spinner 1 because the spinner for nose 4 would not fit propeller B. The change in drag coefficient ΔC_D is a combination of the increment of drag of the body and the change in the propeller efficiency caused by body interference and by the drag of the exposed propeller hub and blade shanks.

In figure 12, the effective ΔC_D caused by the nose shapes is plotted against $1/\sqrt[3]{P_c}$. For small values of $1/\sqrt[3]{P_c}$, the main effect is the change in body drag produced by high velocities over the nacelle; for larger values of $1/\sqrt[3]{P_c}$, the main effect is the change in propeller efficiency.

The preceding fact is illustrated in figure 12(b) in the ΔC_D curve for nose 5 without spinner. This arrangement has the smallest value of ΔC_D for any nose tested with this propeller for values of $1/\sqrt[3]{P_c}$ below 2.0 and the highest value of ΔC_D for values of $1/\sqrt[3]{P_c}$ of 3.4 or more. The fact that the values of ΔC_D up to $1/\sqrt[3]{P_c} = 2.0$ are low shows that the slipstream-drag effect is small. The fact that the values of ΔC_D at $1/\sqrt[3]{P_c} = 3.4$ or more are high shows that the power absorbed by the propeller hub and the blade shanks in the relatively high-velocity air stream of nose 5 without spinner is large.

The addition of spinner 1 to nose 5 decreases the power absorbed by the inner part of the propeller and makes the arrangement of nose 5 with spinner as good as any tested in the high-speed range, except nose 4.

GENERAL DISCUSSION:

The results of tests without propellers show that the increase in the drag coefficient due to replacing a stream-line nose with an open-nose N.A.C.A. cowling is equal to 0.0081. The propeller tests were made with a 10-foot-diameter propeller and a 52-inch-diameter nacelle, which gives a value of $F/S = 0.188$. The maximum power that can be efficiently utilized with a 10-foot-diameter propeller at a speed of 300 miles per hour is approximately 750 horsepower. These conditions give a value of $1/\sqrt[3]{P_c} = 2.68$. From figure 12(b), the value of ΔC_D for nose 1 at $1/\sqrt[3]{P_c} = 2.68$ is 0.0094. This value of ΔC_D includes the effect of the nose opening and the change in the propeller efficiency caused by exposing the propeller hub and the round blade shanks. The change in ΔC_D caused by shielding the hub and the blade shanks with spinner 1 on nose 5 is equal to 0.0033. A similar application of a spinner with nose 1 would result in a reduction of ΔC_D from 0.0094 to approximately 0.008, the value obtained by the drag tests.

From the definition of ΔC_D in terms of propeller efficiency, a ΔC_D of 0.008 gives a change in propeller efficiency of 2.9 percent at $1/\sqrt[3]{P_c} = 2.68$ and $F/S = 0.188$. If the same ΔC_D were applied at the same value of $1/\sqrt[3]{P_c}$ to a 14-foot-diameter propeller and a 52-inch-diameter nacelle, the percentage change of propeller efficiency would be 1.5. This example would apply to a 1,470-horsepower engine and a speed of 300 miles per hour.

This same result may be calculated from the drag results in the following manner. A 52-inch-diameter cowling in an air stream of 300 miles per hour with a drag coefficient of $\Delta C_D = 0.008$ absorbs 22 horsepower. This power amounts to 2.9 percent of the engine power for a 750-horsepower engine or to 1.5 percent for a 1,500-horsepower engine.

As stated previously, about 1 percent of the engine power is required for internal work in cooling the rear of the engine cylinders. Since the open-nose cowling provides sufficient cooling for the front of the cylinders, its aerodynamic power cost should be credited with 1 percent

for this useful work. Thus, only 1.9 percent of the engine power is chargeable to the open-nose cowling at 300 miles per hour for a 750-horsepower engine and 0.5 percent for a 1,500-horsepower engine.

The total percentage of power chargeable to the installation of a radial engine with N.A.C.A. cowling in front of a thick wing or a fuselage is equal to that power chargeable to the nose opening plus the power chargeable to cooling the cylinders. Thus, at 300 miles per hour, this installation cost is 3.9 percent of the engine power for the 750-horsepower engine and 2.5 percent for the 1,500-horsepower engine.

Although the preceding result is extremely important as regards radial-engine installations, it is even more important in its general application to airplane design. The greatest drawback to radial-engine installations, namely, the supposedly high aerodynamic drag of the large frontal area, has been eliminated.

The fact that the power cost of the blunt nose is so markedly affected by the afterbody helps to explain why many test results of cowling installations on airplanes have shown the power cost to be of the order of 25 percent of the engine power. This high power cost means that the nacelles produced some bad flow condition. The test results in this report also explain how some modern airplane-engine installations have given speeds much higher than can be computed from existing cowling-performance data. The installations that gave the high-speed performance were free from bad flow conditions and consequently gave results comparable with those discussed in this report. More exact information on this problem in relation to modern airplanes is an important subject for further research.

CONCLUSIONS

1. The increase in drag of a conventional N.A.C.A. open-nose cowling over that of a streamline nose is greatly affected by the shape of the afterbody. Of the two streamline afterbodies tested, the more streamlined afterbody showed the increment of drag associated with changing

the nose to be about one-fourth of that with the other afterbody.

2. The results show that the drag measurements obtained without the use of the propeller on a neutral afterbody need not be corrected in applying them to the condition of the propeller operating.

3. The results from this investigation indicate that the power cost, in excess of that with a streamline nose, of using an N.A.C.A. cowling in front of a well-designed afterbody to enclose a 1,500-horsepower engine on an airplane with a speed of 300 miles per hour amounts to 1.5 percent of the engine power. To this value must be added 1 percent for the internal work of cooling the rear of the engine cylinders, giving a total installation power cost of 2.5 percent. If the open-nose cowling is credited with 1 percent because it cools the front of the cylinders, the nonuseful power cost of the N.A.C.A. installation amounts to only 0.5 percent of the engine power.

Langley Memorial Aeronautical Laboratory,
National Advisory Committee for Aeronautics,
Langley Field, Va., April 28, 1939.

REFERENCES

1. Theodorsen, Theodore, Brevoort, M. J., and Stickle, George W.: Full-Scale Tests of N.A.C.A. Cowlings. T.R. No. 592, N.A.C.A., 1937.
2. Brevoort, M. J., Stickle, George W., and Ellerbrock, Herman H., Jr.: Cooling Tests of a Single-Row Radial Engine with Several N.A.C.A. Cowlings. T.R. No. 596, N.A.C.A., 1937.
3. Brevoort, M. J., and Joyner, U. T.: Cooling on the Front of an Air-Cooled Engine Cylinder in a Conventional Engine Cowling. T.R. No. 674, N.A.C.A., 1939.
4. Weick, Fred E., and Wood, Donald H.: The Twenty-Foot Propeller Research Tunnel of the National Advisory Committee for Aeronautics. T.R. No. 300, N.A.C.A., 1928.

TABLE I
Results from Tests without a Propeller

Set-up	Nose	Nacelle	C_D (uncorrected for horizontal buoyancy)	C_D	D at $q=25.6$ lb./sq.ft. (lb.)	$C_D - C_{D_0}$	D-D ₀ at $q=25.6$ lb./sq.ft. (lb.)	Remarks
Streamline 1	8	1	0.0861	0.0739	27.9			Streamline shape for set-up 1.
→ solid disk 1	19	1	.1115	.1011	38.2	0.0272	10.3	
→ 1	2	1	.1193	.1089	41.2	.0350	13.3	
→ 1	7	2	.1193	.1085	41.0	.0346	13.1	
→ 1	19	2	.1126	.1013	38.3	.0274	10.4	
→ Streamline 2	4	1	.0710	.0670	25.3			Streamline shape for set-up 2
→ 2	4	1	.0728	.0688	26.0	.0018	.7	Spinner off
→ 2	5	1	.0744	.0709	26.8	.0039	1.5	With spinner 1
→ 2	5	1	.0728	.0693	26.2	.0023	.9	
→ 2	3	1	.0802	.0762	28.8	.0093	3.5	
→ 2	3	1	.0773	.0733	27.7	.0063	2.4	With spinner 1
→ 2	1	1	.0809	.0751	28.4	.0081	3.1	
→ 2	2	1	.0840	.0780	29.5	.0110	4.2	

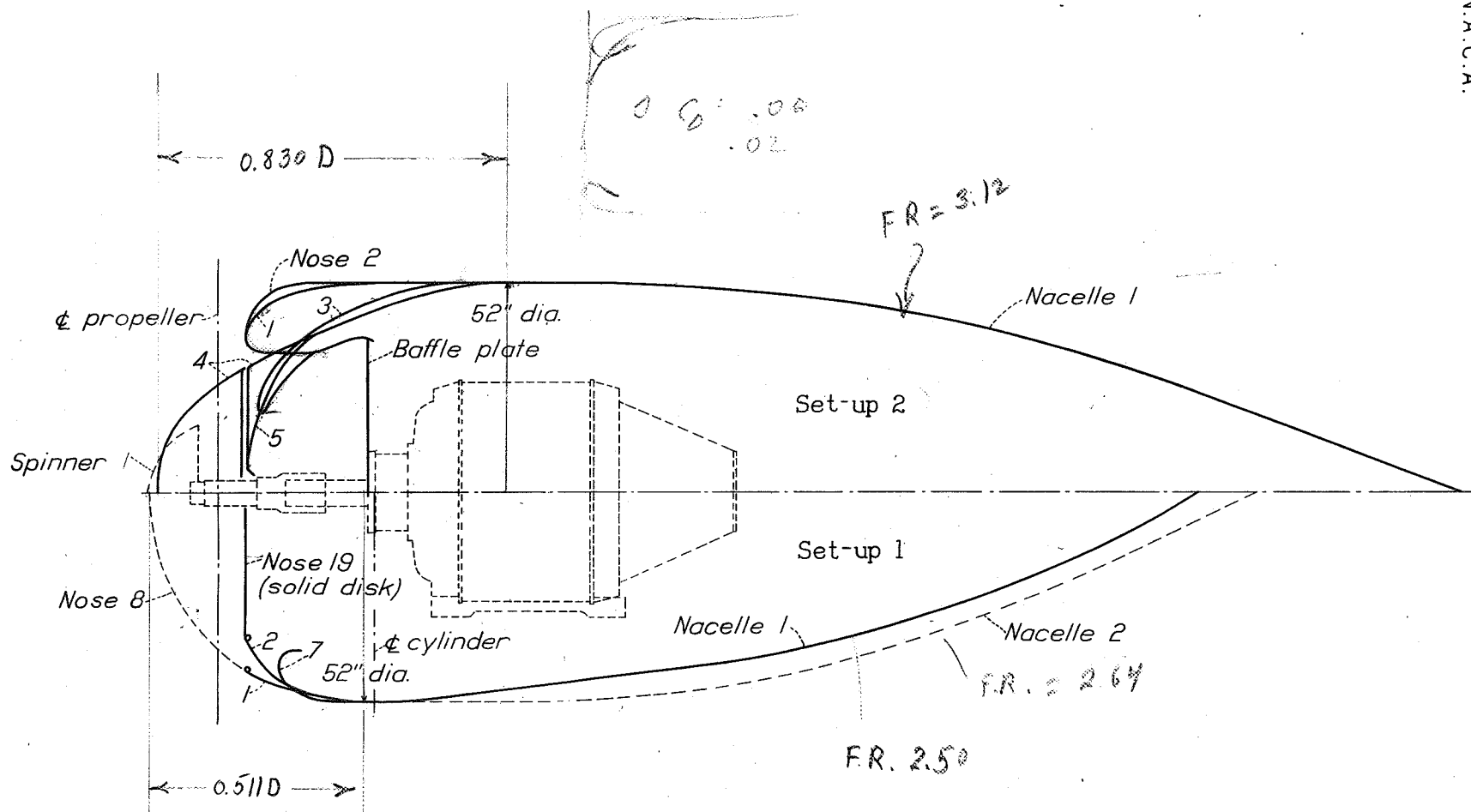


Figure 1.- Line drawing of the test arrangements.

N.A.C.A.

Figs. 2, 3

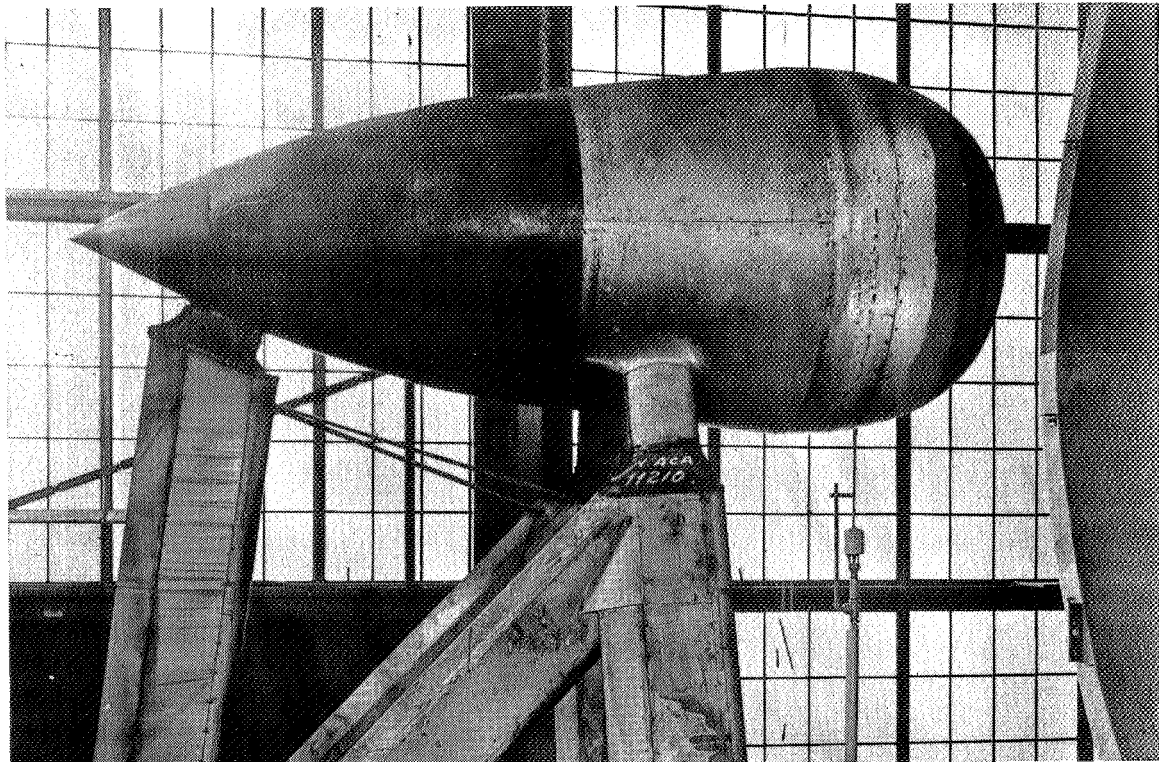


Figure 2.- The streamline shape used with set-up 1.

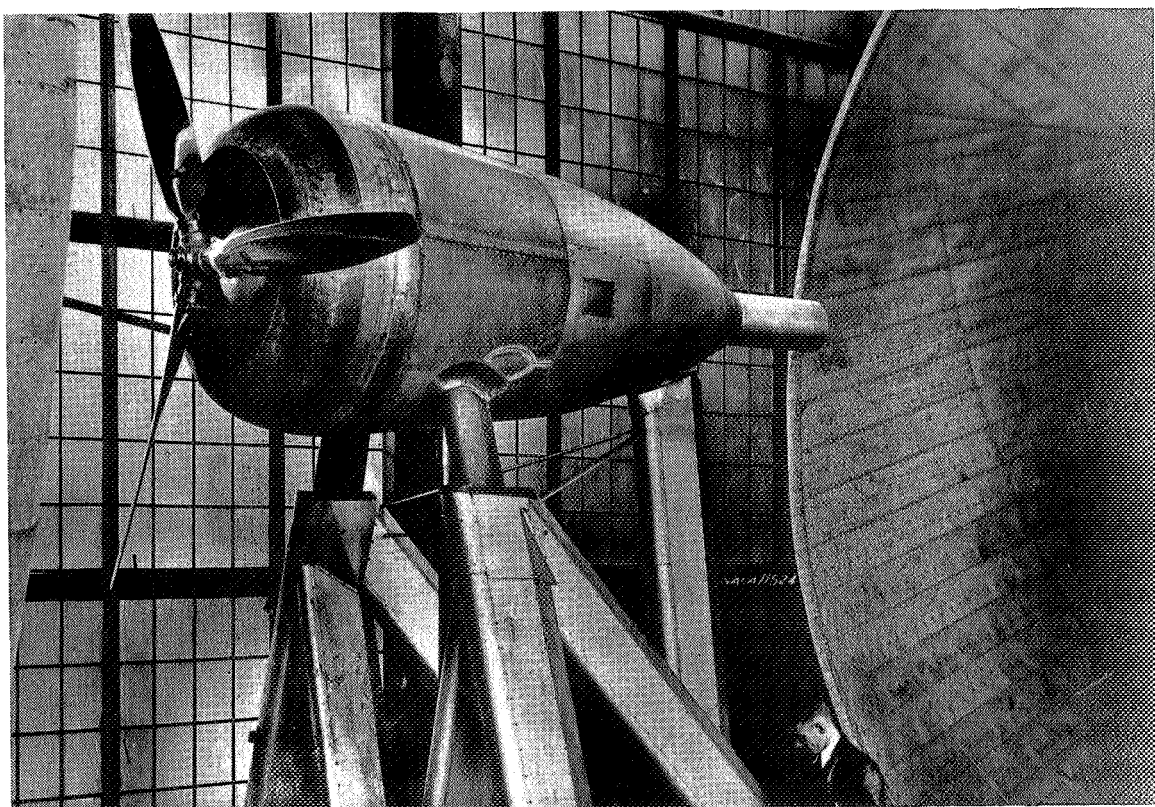


Figure 3.- Set-up 1, nose 2, nacelle 1 with propeller and tail pump in place. The results discussed in this report were obtained with an afterbody having a pointed tail, as shown in fig. 1.

N.A.C.A.

Figs. 4, 5

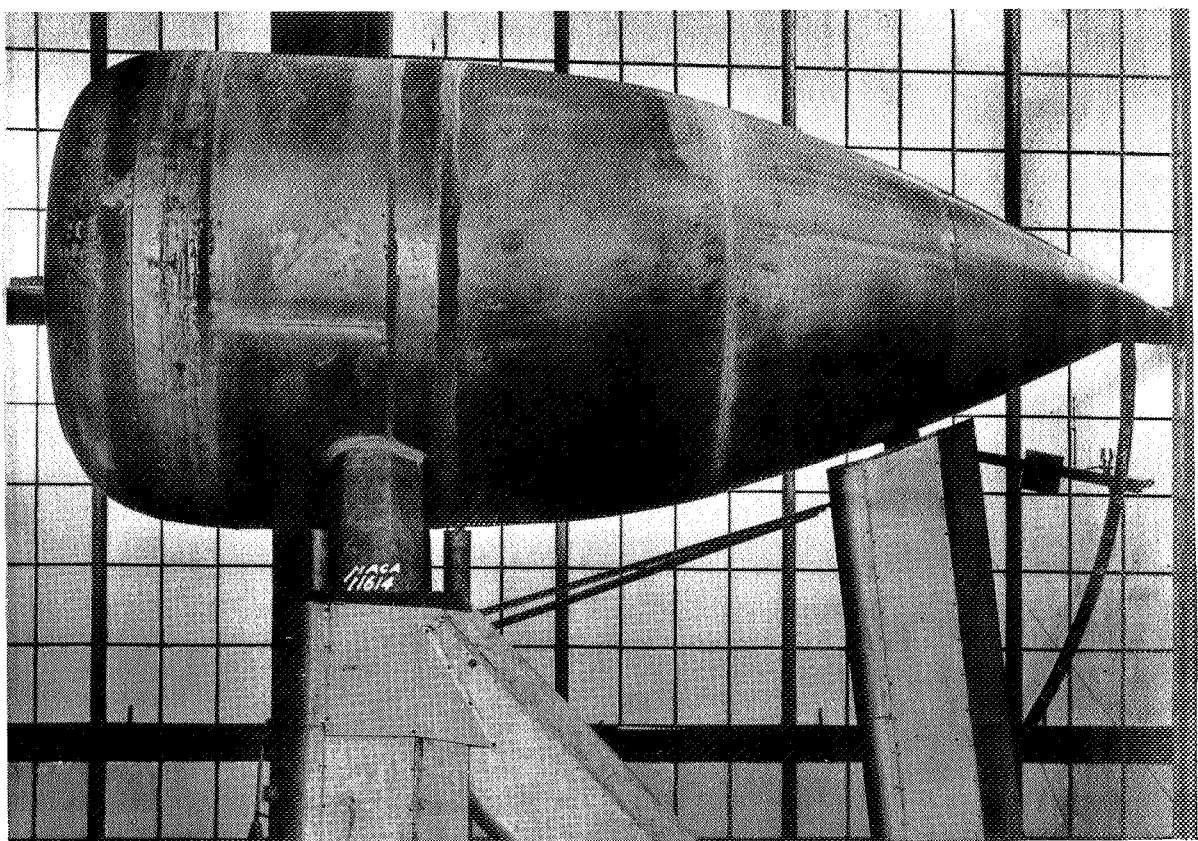


Figure 4.- Side view of set-up 1, nose 2, nacelle 2.

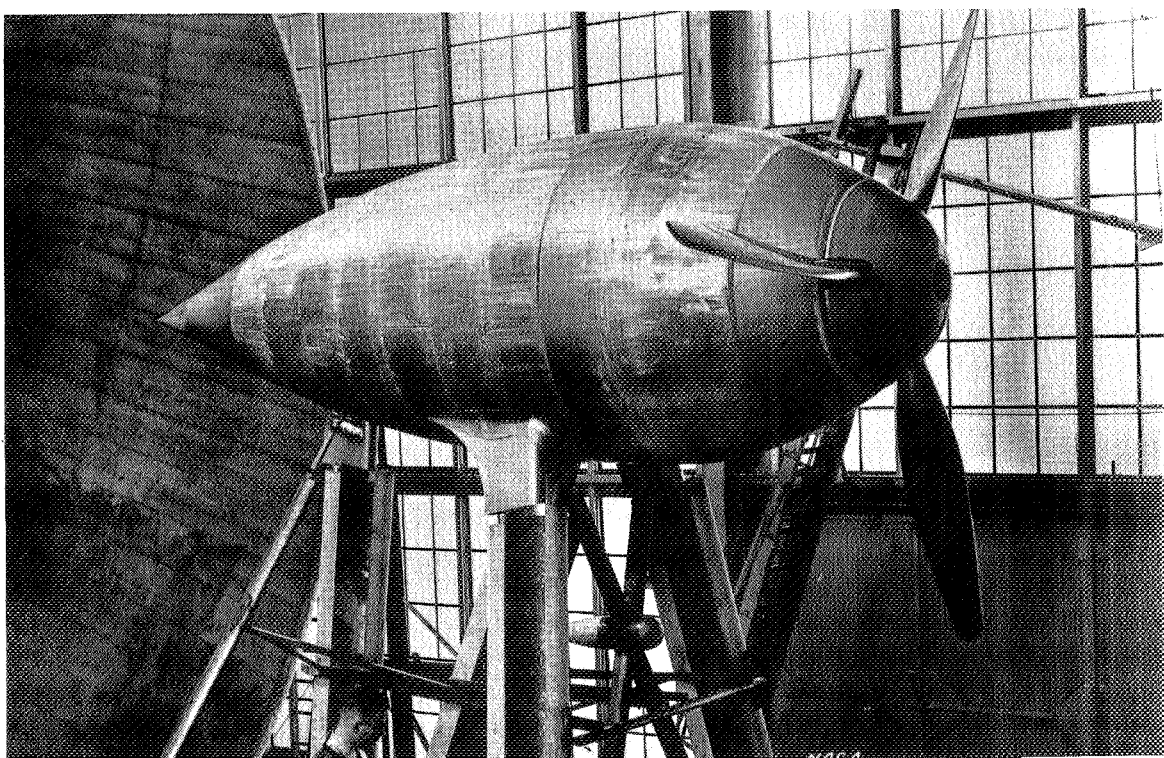


Figure 5.- The streamline shape used with set-up 2 with the propeller in place.

N.A.C.A.

Figs. 6,7

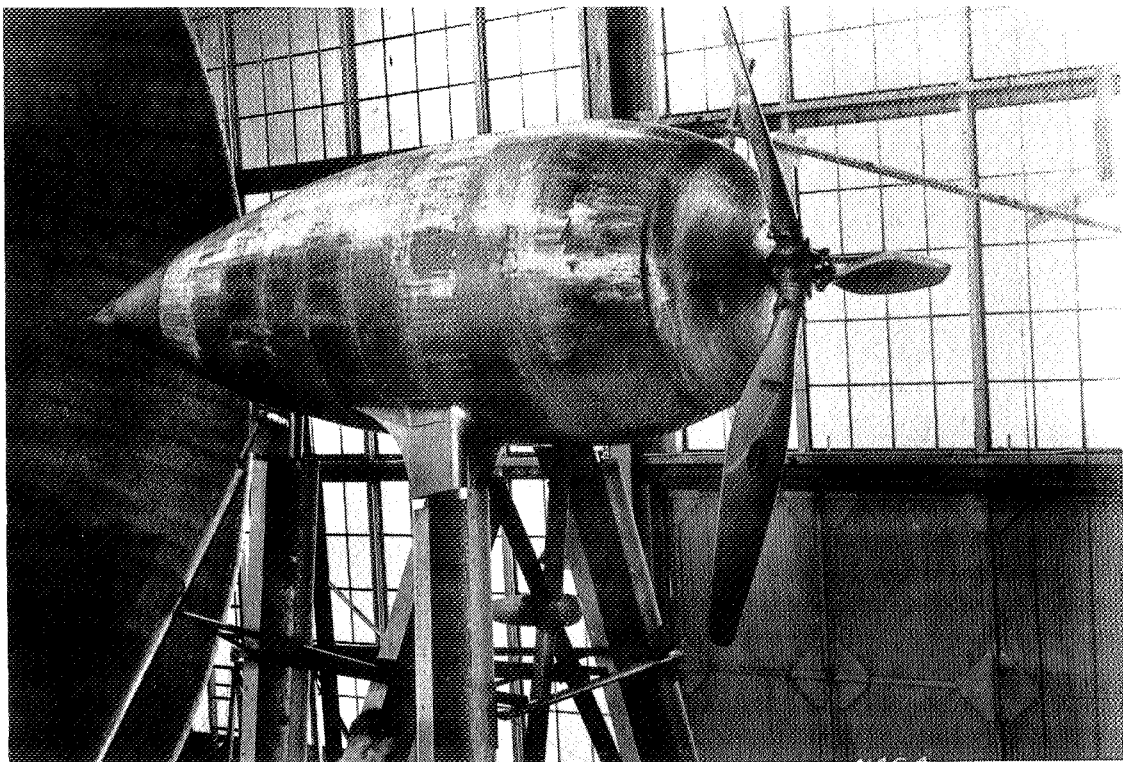


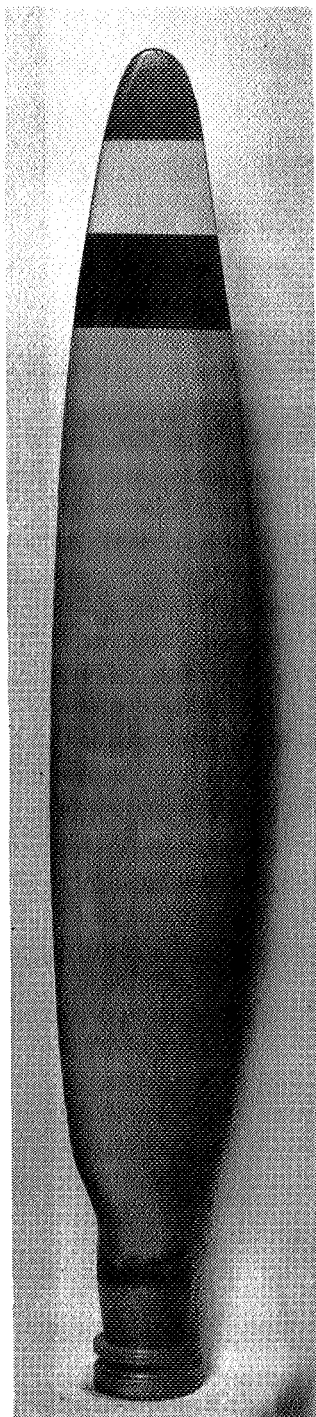
Figure 6.- Set-up 2, nose 5, nacelle 1 with propeller in place.



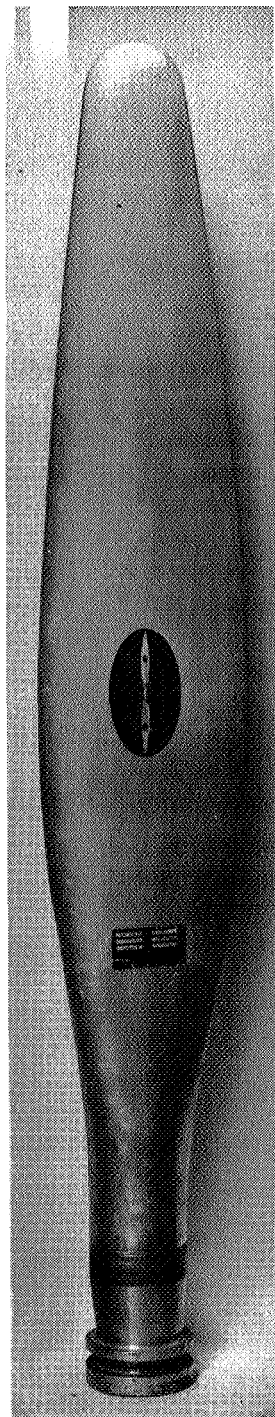
Figure 7.- Set-up 2, nose 1, nacelle 1 with a $1\frac{1}{2}$ -inch slot opening.
The results discussed in this report were obtained with
all slots closed and faired.

N.A.C.A.

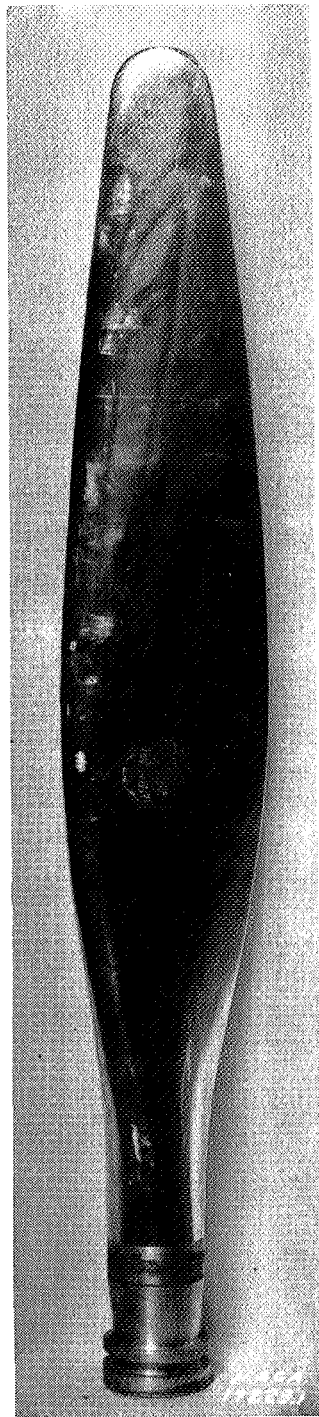
Fig. 8



B



C



C_x

Figure 8.- One blade of each of the three 10-foot-diameter
3-blade propellers used.

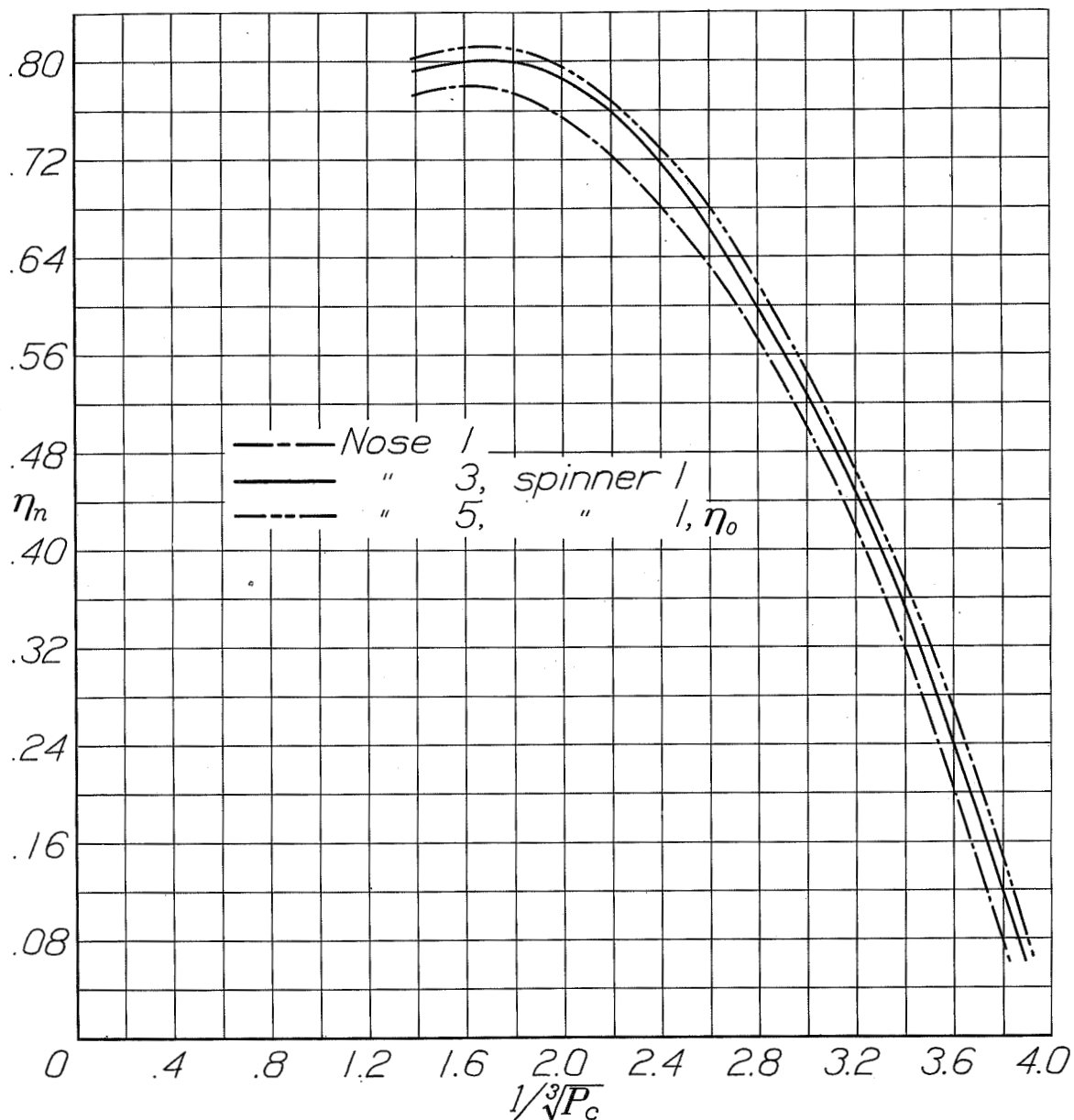


Figure 9.- Net-efficiency envelopes for noses 1, 3, and 5 with propeller B.

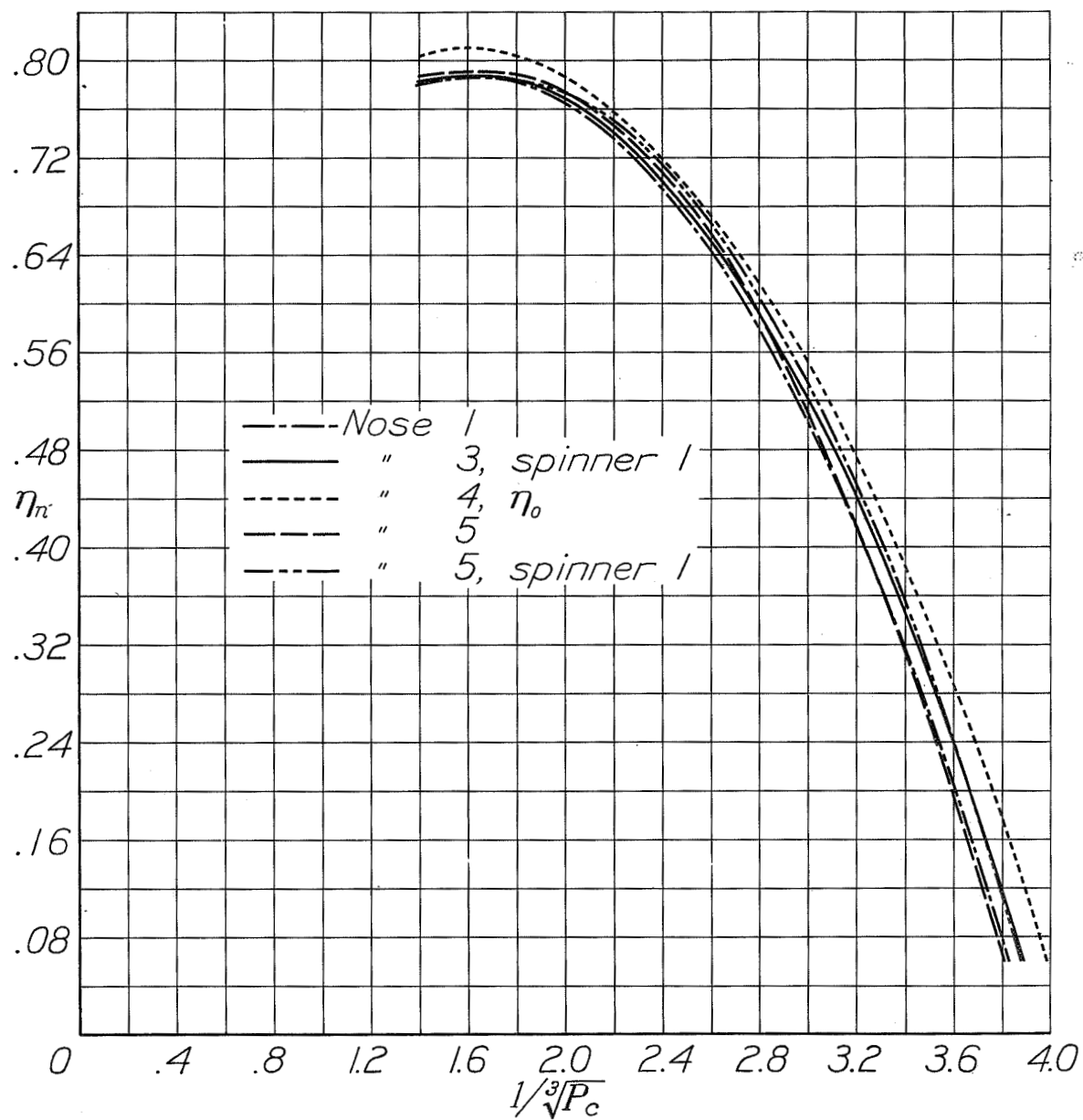


Figure 10.- Net-efficiency envelopes for noses 1, 3, 4, and 5 with propeller C.

N.A.C.A.

Fig. 11

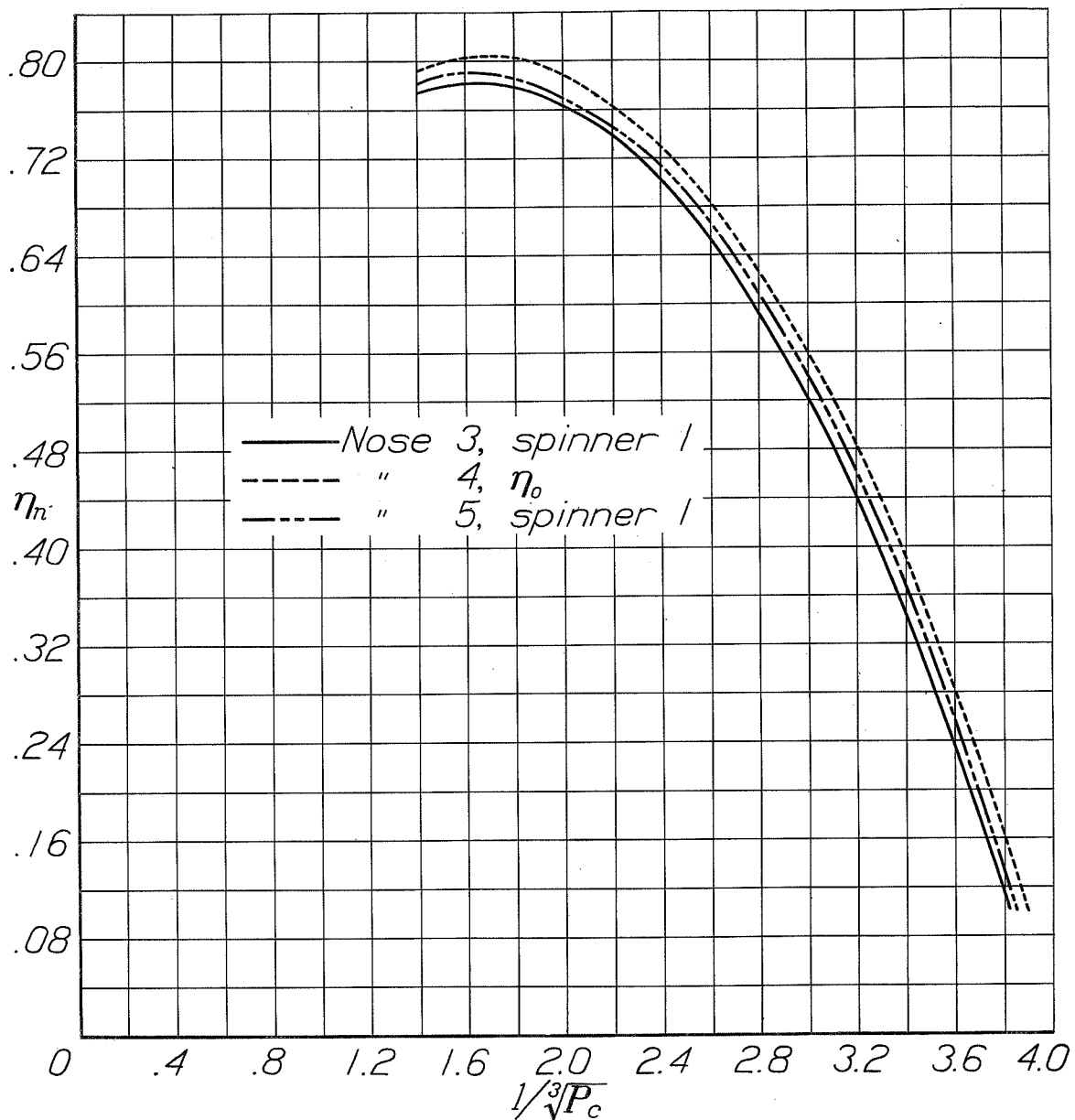
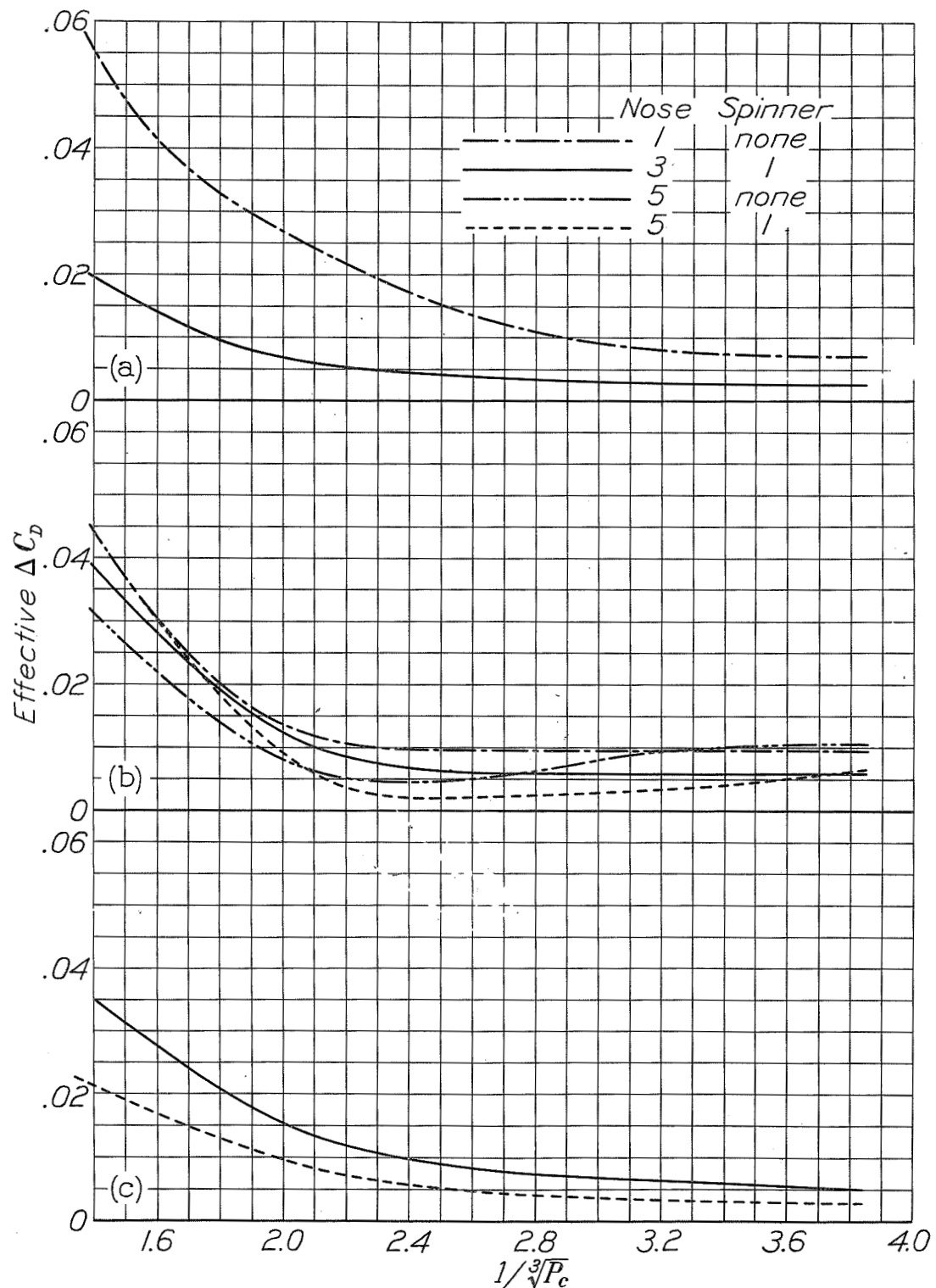


Figure 11.- Net-efficiency envelopes for noses 3, 4, and 5 with propeller C_x .



(a) Noses 1 and 3; nose 5 with spinner 1 used as basis. Propeller B.

(b) Noses 1, 3 and 5; nose 4 used as basis. Propeller C.

(c) Noses 3 and 5; nose 4 used as basis. Propeller C_x.

Figure 12.- The variation of the effective ΔC_D with $1/\sqrt[3]{P_c}$ obtained from the differences in the net efficiencies.